

Supplementary Information for

A pan-mammalian map of interhemispheric brain connections predates the evolution of the corpus callosum

Rodrigo Suárez^{a,1}, Annalisa Paolino^a, Laura R. Fenlon^a, Laura R. Morcom^a, Peter Kozulin^a, Nyoman D. Kurniawan^b, and Linda J. Richards^{c,1}

Rodrigo Suárez and Linda Richards
Email: r.suarez@uq.edu.au or richards@uq.edu.au.

This PDF file includes:

Materials and Methods
Figures S1 to S9 and corresponding legends
Table S1
Captions for Movies S1 to S3
References

Other supplementary materials for this manuscript include the following:

Movies S1 to S3

Materials and Methods

Animals

All animal procedures, including breeding in captivity, were approved by The University of Queensland Animal Ethics Committee and the Queensland Government Department of Environmental and Heritage Protection, and followed the Australian Code for the Care and Use of Animals for Scientific Purposes (National Health and Medical Research Council, 8th edition, 2013), as well as international guidelines on animal care and welfare to minimize animal discomfort. Two adult platypus brains (*Ornithorhynchus anatinus*) fixed in formalin (i.d. 819 and 918) came from the collection of Prof. John Nelson held in the Australian National Wildlife Collection, Commonwealth Scientific and Industrial Research Organisation (CSIRO, Canberra). Fat-tailed dunnarts were bred in captivity, as described previously (1). Brains were collected after transcardial perfusion of saline (0.9%) and formalin (4% paraformaldehyde, PFA).

***Ex vivo* magnetic resonance imaging**

Fixed brains of platypus (n = 2) and dunnarts (n = 3) were incubated for four days in the contrast agent gadopentetate dimeglumine (Magnevist, Bayer) at 0.25% v/v in 1M phosphate buffer saline (PBS), pH 7.4. For dunnart brains, magnetic resonance imaging was performed using a 16.4 T micro-imaging spectrometer (Bruker Ultrashield Plus Avance I; 89 mm bore diameter, Paravision 5.1) and a

15 mm surface acoustic wave coil (M2M Imaging). Three-dimensional high-resolution structural images were acquired using fast low angle shot (FLASH) with the following parameters: echo time (TE)/repetition time (TR) = 12/50 ms, flip angle (FA) = 30°, one excitation, field of view (FOV) = 1.74 x 1.2 x 0.8 cm, 30 μm isotropic resolution, and acquisition time of 40 min. High angular resolution diffusion imaging (HARDI) was acquired with the same FOV, using three-dimensional diffusion-weighted spin echo sequence of TE/TR = 20/400 ms, diffusion gradient δ/Δ = 2.5/12.5 ms, b-value = 5000 s/mm^2 , 30 diffusion encoding directions, 100 μm isotropic resolution, and acquisition time of 16 hours. For platypus brains, one sample was acquired at 16.4T using 3D FLASH with TE/TR = 6/50 ms, FA = 30°, four excitations, FOV = 3.24 x 2.77 x 2.30 cm, 80 μm isotropic resolutions, and acquisition time of 2.5 h. Three-dimensional HARDI was acquired with the same FOV using TE/TR = 21/200 ms, δ/Δ = 2.5/12.5 ms, b-value = 3000 s/mm^2 , 30 diffusion encoding directions at 180 μm isotropic resolution. A second, slightly larger platypus brain sample was scanned at 9.4 T (Bruker Biospec Avance III, 300 mm bore diameter, Paravision 5.1) using a 40 mm rat head volume coil. Structural imaging was acquired using a three-dimensional rapid acquisition with relaxation enhancement (RARE) sequence, with TE/TR = 24/400 ms, RARE factor = 4, one excitation, FOV = 4.2 x 3.3 x 3.6 cm at 150 μm isotropic resolution, and acquisition time of 52 min. Three-dimensional HARDI was acquired using TE/TR = 250/30 ms, δ/Δ = 4/20 ms, b-

value = 4000 s/mm², 30 diffusion encoding directions at 300 μm isotropic resolution, and acquisition time of 13.5 h.

Tractography reconstructions

Diffusion MRI datasets were processed using HARDI/Q-ball reconstruction and tractography streamlines were generated using the fiber assignment by continuous tracing (FACT) method within the diffusion toolkit of TrackVis program (www.trackvis.com). Briefly, dunnart brain structural scans were examined in the three planes and a spherical region of interest (ROI) was placed within the center of the anterior commissure and used as a seeding point to visualize interhemispheric tracts (radius = 4.75, corresponding to 142.5 μm, and coordinates = 50, 89, 157), and inclusion tracts were generated with smaller color-coded ROIs (radius = 2, *i.e.* 60 μm) at the following coordinates: olfactory bulb (56, 109, 186), entorhinal cortex (47, 26, 121), frontal cortex (85, 76, 187), cingulate/motor cortex (90, 77, 156), primary somatosensory cortex (S1) hindlimb field (90, 77, 156), S1 mandible field (89, 58, 138), and S1 mystacial whisker field (78, 46, 139), as shown in Fig. 2A. The same procedure was done in platypus with the following parameters: anterior commissure (radius = 6, *i.e.* 480 μm, coordinates = 77, 82, 126) and inclusion ROIs (radius = 1.5, *i.e.* 120 μm) in the piriform cortex (85, 92, 151), rostral somatosensory cortex (R) upper-bill (70, 104, 148), S1 upper-bill (85, 111, 134), R head-shield (85, 123, 119), S1 central upper-bill (75, 129, 103), and entorhinal cortex (93, 106, 86), as shown in Fig. 3

A and B. Confirmation of segregated domains was done by generating color-coded tracts after drawing individual, non-contiguous, two-dimensional ROIs with the hand-draw function in TrackVis, at the midsagittal plane of different dunnart and platypus brains (Figs. 2 B and C, and 3 C and D). Supplementary figures S1-S3 and videos S1-S3 of HARDI tractography in both species were made following the aforementioned methods.

***Ex vivo* carbocyanine injections**

For histological confirmation of segregated tracts, we performed double injections with carbocyanine crystals, DiI and DiD (1,1'-dioctadecyl-3,3,3',3'-tetramethylindocarbocyanine perchlorate, and 1,1'-dioctadecyl-3,3,3',3'-tetramethylindocarbocyanine, 4-chlorobenzenesulfonate salt, respectively; Invitrogen, Thermo Fisher Scientific) in formalin-fixed dunnart brains. Briefly, carbocyanine crystals were sonicated and small fragments were placed into one of two regions within the same hemisphere using a pulled glass micropipette. Brains were incubated in 4% PFA at 4°C for one week, and then transferred to a 38°C oven for at least 7 months to ensure axonal transport. We then embedded the brains in 3.4% agarose and obtained 50 µm coronal sections using a vibratome (VT1000S, Leica Biosystems). Sections were mounted, stained for 10 min with DAPI (0.1% 4',6-Diamidino-2-phenylindole dihydrochloride; Invitrogen, Thermo Fisher Scientific), washed in 1M PBS, cover slipped and imaged within 48 h.

In-pouch electroporation of dunnart joeys

Female dunnarts were anaesthetized as described above, and joeys examined inside the pouch. Electroporation of cortical neurons in postnatal dunnarts attached to the teat was performed inside the pouch as described previously (2). A small amount (0.5-1 μ L) of a 1 mL/mg DNA solution of pCAG-eYFP plasmid was injected into the lateral ventricle, followed by electroporation with forceps-type electrodes (Nepa Gene), which delivered five 100 ms square pulses of 30-35 V at 1Hz (ECM 830, BTX, Harvard Bioscience). Joeys were collected around 50 postnatal days, and perfused as described above.

Immunofluorescence and microscopy

Brains sections were mounted and stained for DAPI alone (dye injections), or combined with immunohistochemistry. The primary antibodies were chicken anti-Gfp (1:750, ab13970, Abcam), goat anti-TdTomato (1:1000, AB8181-200, SICGEN), rabbit anti-Nurr1 (1:500, sc-991, Santa Cruz Biotech), rat anti-Ctip2 (1:500, ab18465, Abcam), with the corresponding secondary fluorescent antibodies (Alexa Fluor 488/555/568/647; Invitrogen, Thermo Fisher Scientific). Images were obtained using an upright microscope (Axio-Imager Z1, Zeiss) fitted with an AxioCam MRm camera, and captured with Zen software (Zeiss). Higher magnification images were obtained using an inverted microscope (TiE, Nikon)

with a spinning disk confocal module (Diskovery, Andor), fitted with a sCMOS camera (Andor Zyla 4.2) and captured with NIS software (Nikon).

***In vivo* stereotaxic injections of retrograde tracers**

We performed 17 injections of retrograde tracers (Dil and/or DiI, 10 mg/mL dissolved in dimethyl sulfoxide, and/or cholera toxin beta-subunit conjugated with AlexaFluor 555 or 647, 5 mg/mL in PBS; Invitrogen, Thermo Fisher Scientific) in 13 dunnarts *in vivo*. Animals were anaesthetized with 5% isoflurane in medical oxygen, delivered at 200mL/kg/min, placed in a mouse stereotaxic apparatus (Stoelting) and kept under 2-5% isoflurane through a nose mask. A pulled glass pipette was used to inject the dyes via a picospritzer (Parker Hannifin).

Coordinates with respect to Bregma were recorded and cortical areas were assessed by comparing a brain atlas of the stripe-faced dunnart (*Sminthopsis macroura*) (3) with histology. Brains were collected after 7 days by transcardial perfusion of 0.9% NaCl followed by 4% PFA, and sectioned coronally as indicated above.

Cell-level circuit mapping

The pattern of contralateral connections was mapped at single-cell resolution in dunnart brains after injections of retrograde tracers into the opposite hemisphere. To detect the injection sites, coronal sections of dunnart brains were visualized and imaged using an upright microscope (Axio-Imager Z1, Zeiss) fitted with an

AxioCam MRm camera and captured with Zen software (Zeiss). The hemispheres contralateral to the injection sites were then imaged at high resolution using an inverted Nikon TiE microscope (Nikon) with a Discovery spinning disk confocal module (Spectral Applied Research), fitted with a sCMOS camera (Andor Zyla 4.2) and captured with NIS software (Nikon). Experiments in which the injection sites penetrated the white matter or the ventricles, as well as cases where fewer than 80% of brain areas could be quantified, were excluded from the analyses. We manually curated, based on fluorescent cell body morphology, and counted a total of 34,005 contralaterally projecting neurons from 17 well-defined injections in 13 animals. Coronal sections counterstained with DAPI were mapped onto a 10 section template, including all cortical regions, based on an atlas of a related species (*S. macroura*) (3). Labeled cells were counted per area and section by investigators blind to the position of the contralateral injections. A summary of individual experiments is presented in supplementary Table S1. To generate the connectivity matrix in Fig. 4B, we calculated the percentage of retrogradely labeled cells across eight regions per experiment, and averaged experiments with comparable injection sites grouped into seven sites as indicated. In double-injection experiments (Fig. 7), cells were counted at the medial and lateral extents of the contralateral hemisphere having incorporated either one or both tracers. Statistically significant differences were considered as $P < 0.05$, using two-tailed Student's t-tests (for cortical area differences in homotopic, heterotopic and branched projections, Fig. 7E), and

one-way ANOVA (for inter-layer differences in commissural neuron cell counts, Fig. S4) using Prism 7 (GraphPad).

Supplementary Figures

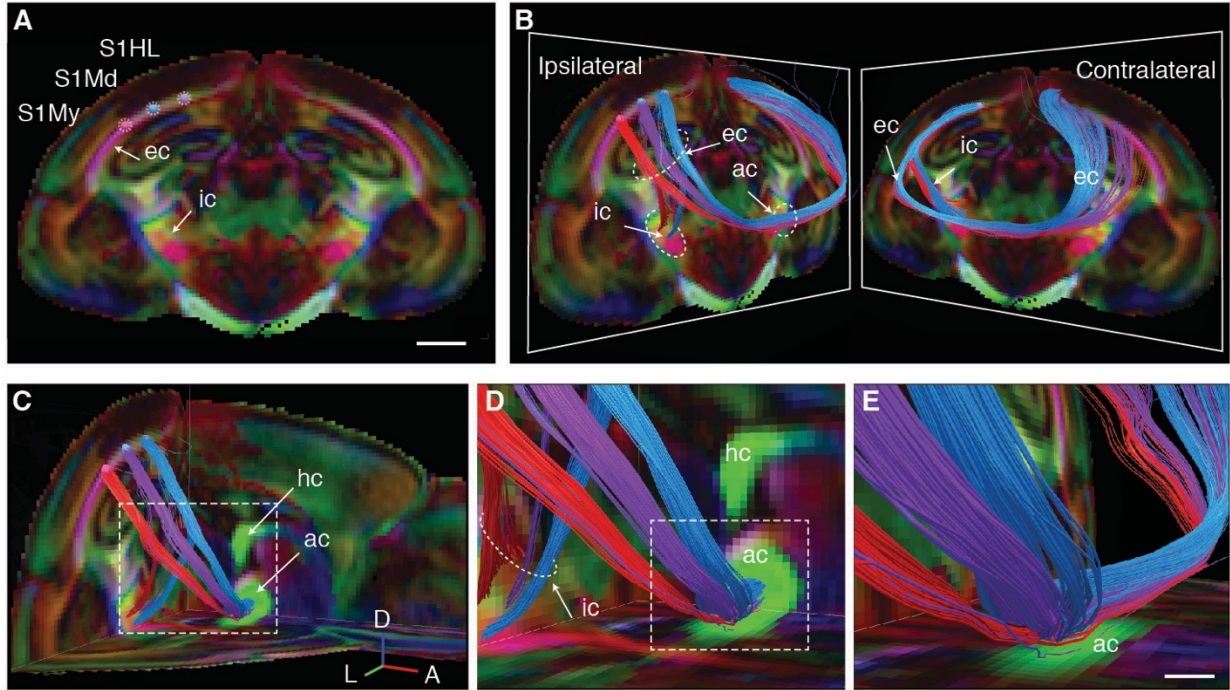


Fig. S1. Intra- and extra-cortical fibers are topographically arranged in dunnarts. (A) Diffusion tensor imaging of a fixed dunnart brain showing three adjacent regions of interest (ROIs) within the primary somatosensory cortex (S1) hindlimb (S1HL), mandibular (S1Md), and mystacial (S1My) subfields. ec, external capsule; ic, internal capsule. (B) Color-coded tracts generated from the ROIs in A seen from ipsilateral and contralateral views reveal axonal segregation of homotopic circuits between hemispheres via the anterior commissure and external capsules, as well as cortical-subcortical topography via the internal capsule. (C and D) The same brain viewed with coronal, horizontal and midsagittal planes showing the point of crossing within the anterior commissure (ac), segregation of fibers within the internal capsule (ic), and the relative position of the hippocampal commissure (hc). (E) Inset from D without the mid-sagittal

plane, showing the contralateral topography of fibers. Scale bars: 1 mm in *A*, 200 μm in *E*.

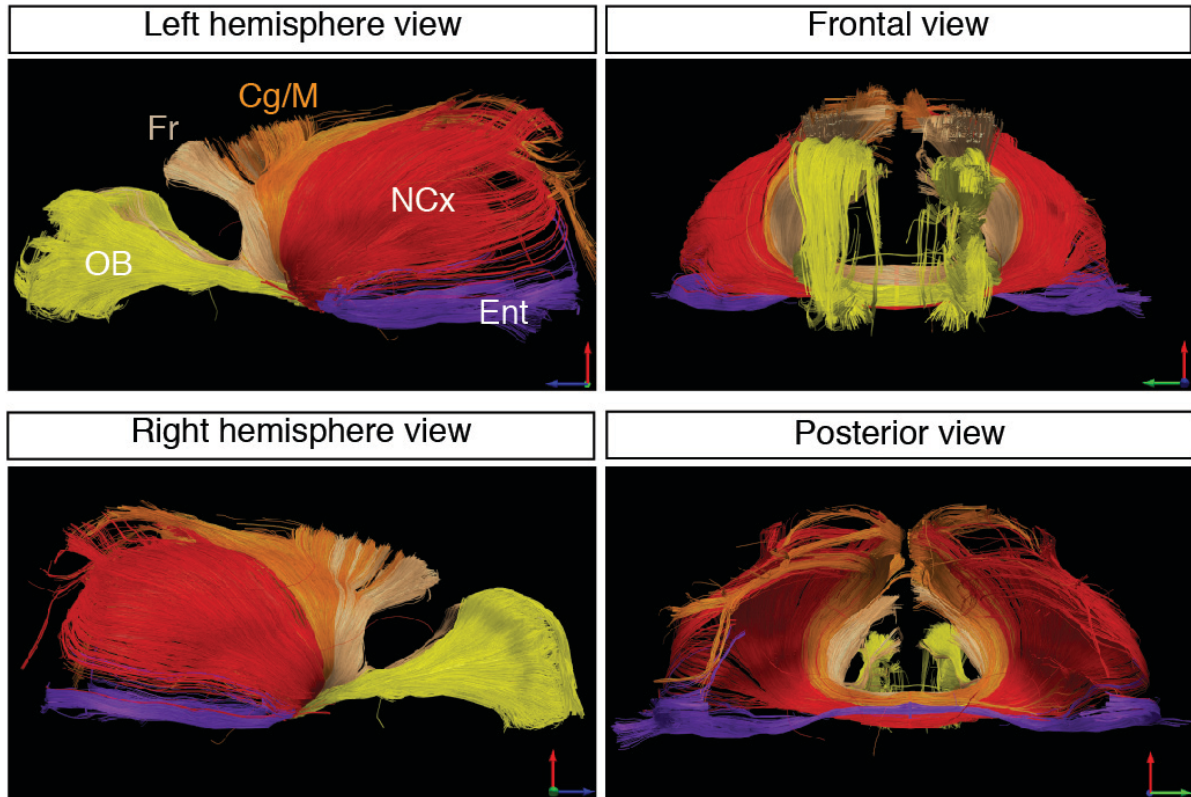


Fig. S2. Homotopic fields can be reconstructed from the mid-sagittal anterior commissure in dunnarts. At least five color-coded homotopic domains can be generated by parcellation of the mid-sagittal anterior commissure as shown in Fig. 1D, including the olfactory bulbs (OB, yellow), frontal cortices (Fr, beige), cingulate and motor regions (Cg/M, orange), and bulk neocortical (NCx, red) and entorhinal cortices (Ent, purple). Views from the left, front, right and back.

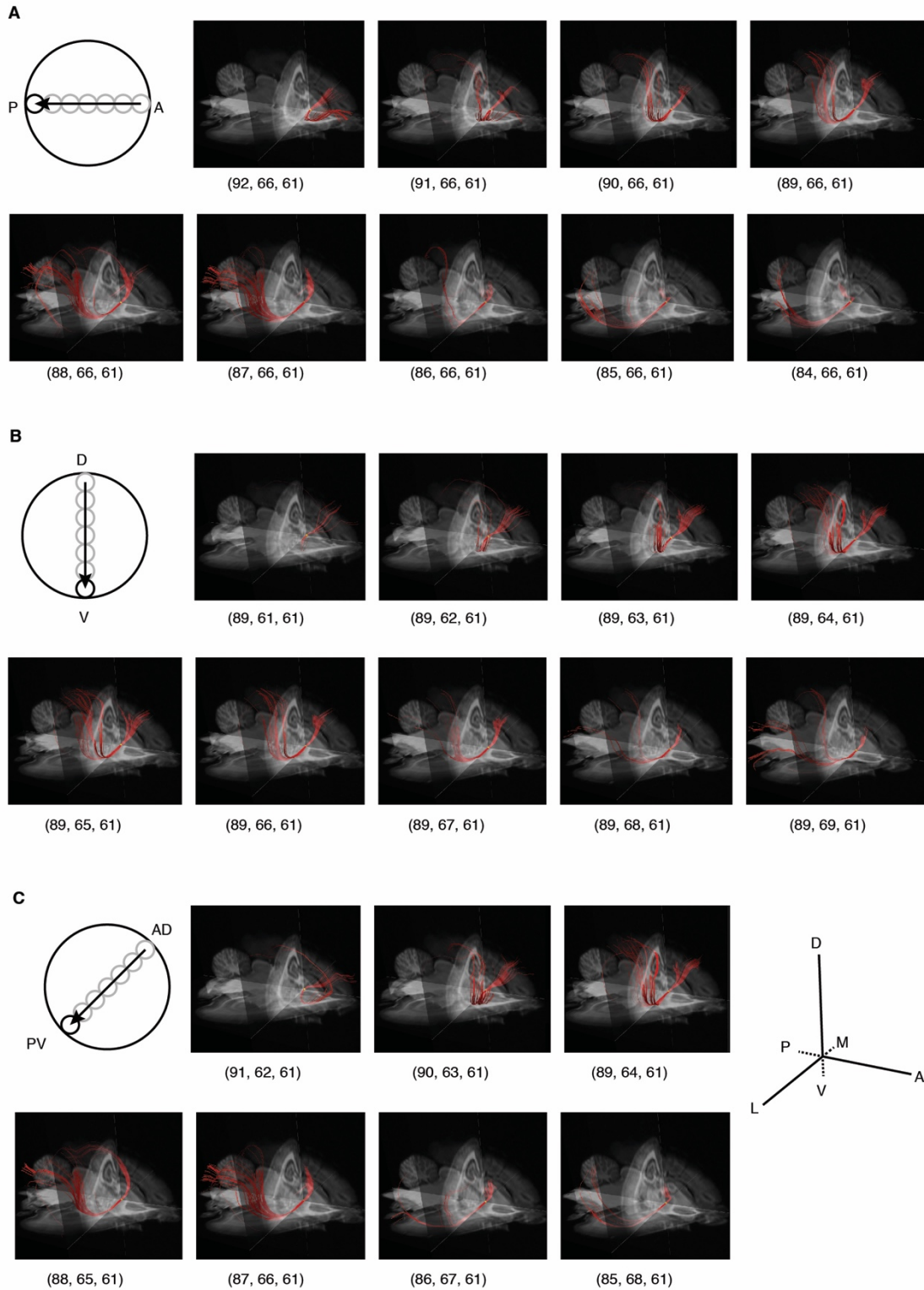


Fig. S3. Segregation of homotopic of fibers within the anterior commissure of platypus.

(A) Movement of a small region of interest (ROI) in seven steps along the antero-

posterior axis (schematics on left) generates tracts in red in the corresponding images on the right (ROI in yellow, coordinates below each panel, see axes in *C*). (*B*) Same procedure as in *A*, but moving the ROI along dorso-ventral equidistant steps. (*C*) Movement of the ROI in the oblique antero-dorsal (AD) to postero-ventral (PV) axis generates the tracts shown on the right. A, anterior; D, dorsal; L, lateral; M, medial; P, posterior; V, ventral.

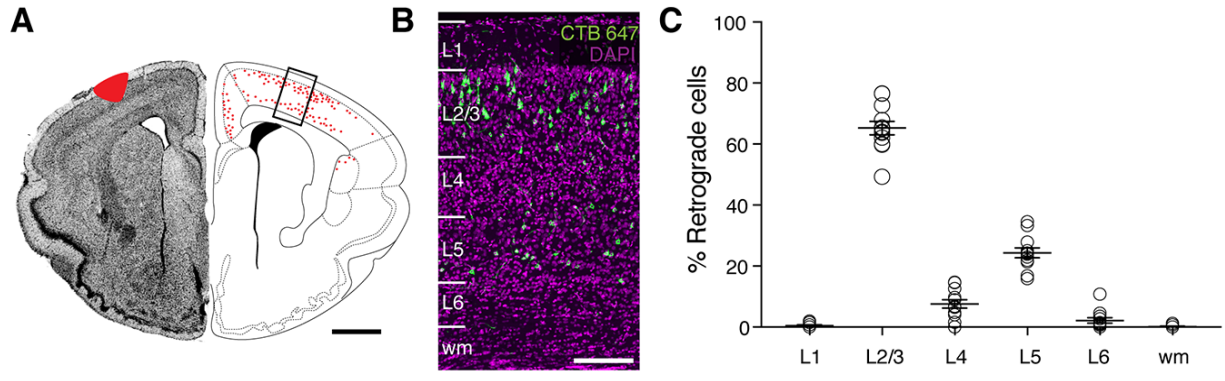


Fig. S4. Layer distribution of commissural neurons in dunnarts. (A) Injections of retrograde tracers into primary sensory areas (e.g., S1 and V1) result in contralaterally labelled neurons located prominently in layers (L) 2/3 and 5 (B). (C) Quantification of the relative percentages of retrogradely labelled neurons across cortical layers after injections in homotopic contralateral areas in four animals. Data indicated as mean \pm SEM. Scale bar: 1 mm in A, 200 μ m in B.

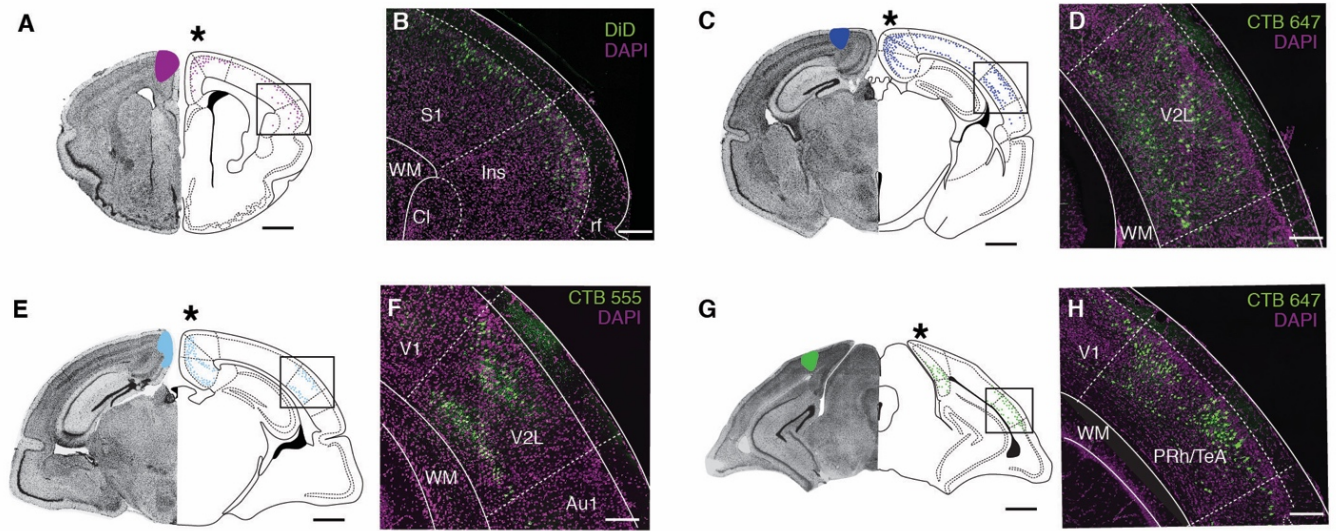
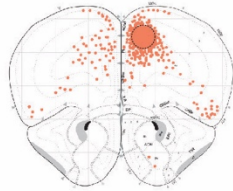


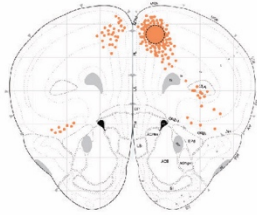
Fig. S5. The medial cortices of dunnarts receive inputs from heterotopic regions of the contralateral neocortex. Four representative cases of medial injections at different antero-posterior extents are shown in *A*, *C*, *E*, and *G*, and insets of the contralateral neocortex in *B*, *D*, *F* and *H*. Homotopically projecting neurons are indicated by asterisks. Cl, claustrum; Ins, insular cortex; PRh/TeA, perirhinal/temporal association cortex; rf, rhinal fissure; S1, primary somatosensory cortex; V1, primary visual cortex; V2L, lateral field of the secondary visual cortex; WM, white matter. Scale bars: 1 mm in *A*, *C*, *E*, and *G*; 250 μm in *B*, *D*, *F* and *H*.

A Unilateral injection site, animal i.d.
Antero-posterior extent from Bregma

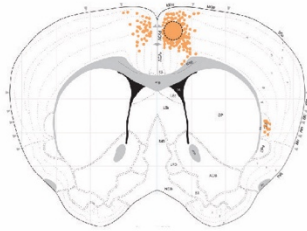
ACAd, SW110614-04
Bregma 2.145 mm



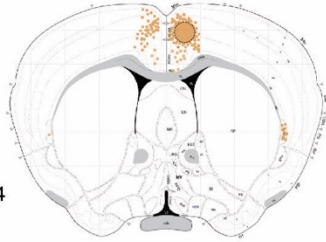
ACAd, SW110613-01
Bregma 1.745 mm



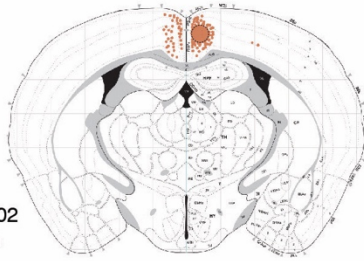
ACAd, SW110614-01
Bregma 0.745 mm



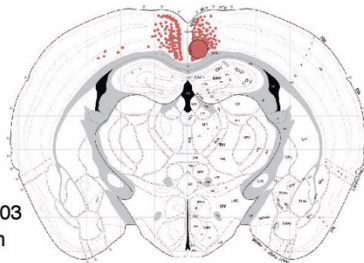
ACAd, SW110613-04
Bregma 0.345 mm



RSPv, SW120525-02
Bregma -1.255 mm



RSPv, SW110614-03
Bregma -1.455 mm



B Retrogradely labelled cell bodies at the level of the claustrum
Bregma 1.545 mm Bregma 1.345 mm

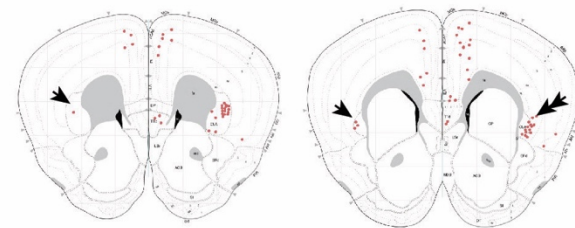
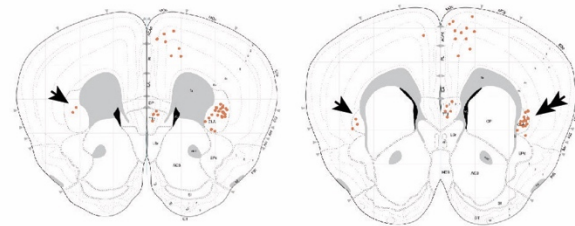
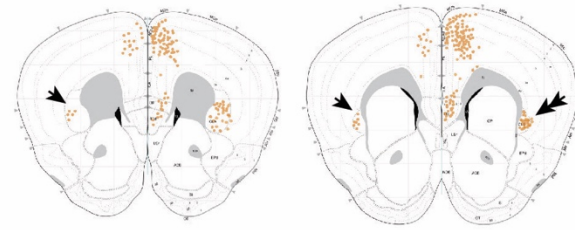
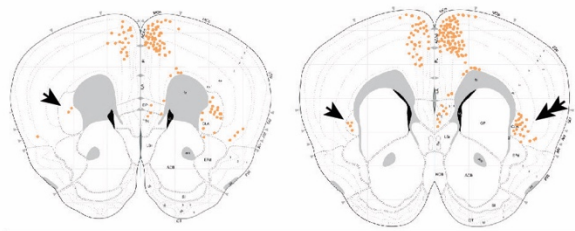
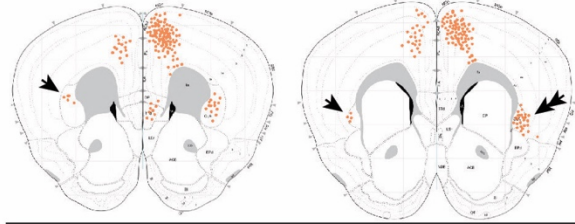
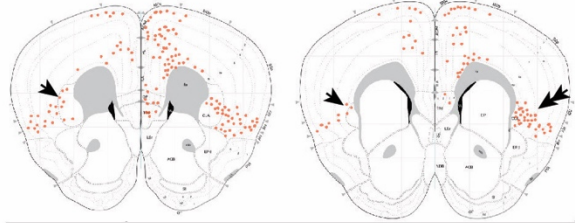


Fig. S6. The claustrum of mice sends ipsilateral and contralateral long-range projections to the medial cortices. (A) Six representative cases of retrograde tracer injection experiments (Fluorogold or cholera toxin B) into the medial cortices (ACAd, anterior cingulate area dorsal; RSPv, retrosplenial cortex ventral) of mice along the antero-posterior axis (injection sites circled and color-coded). (B) Retrogradely labeled cell bodies from each experiment in A, at the level of the claustrum showing contralateral (arrowheads) and ipsilateral (double arrowheads) heterotopic circuits. Courtesy of www.mouseconnectome.org. Scale bar 2 mm.

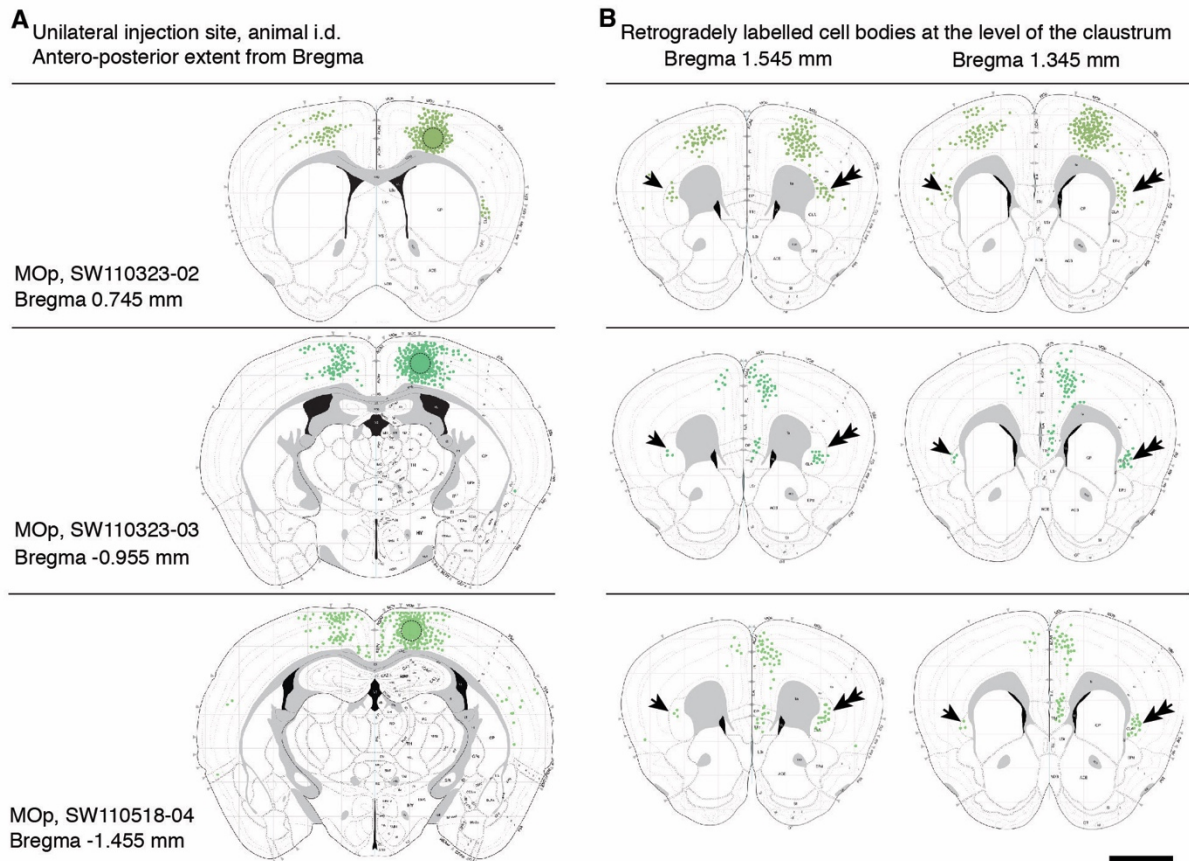


Fig. S7. Long-range heterotopic projections from the mouse claustrum include both motor cortices. (A) Three representative cases of retrograde tracer injections (Fluorogold or cholera toxin B) into the motor cortices (MOp, posterior motor cortex) of mice along the antero-posterior axis (injection sites circled and color-coded). (B) Retrogradely labeled cell bodies from each experiment in A, at the level of the claustrum showing contralateral (arrowheads) and ipsilateral (double arrowheads) heterotopic circuits.

Courtesy of www.mouseconnectome.org. Scale bar 2 mm.

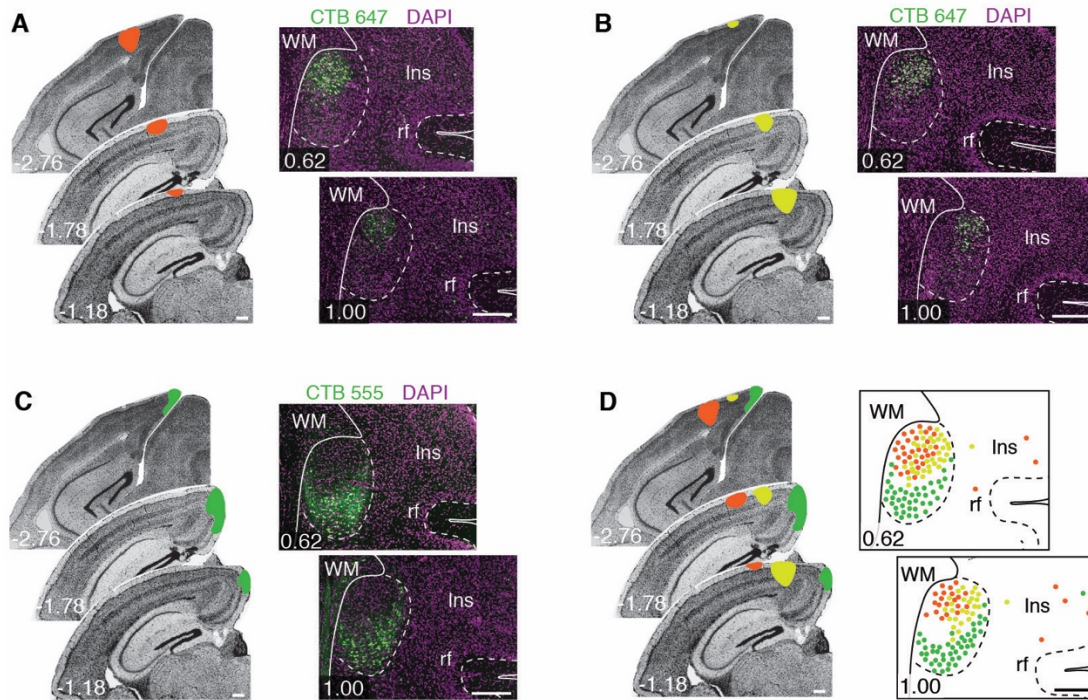


Fig. S8. Contralateral claustrum-cortical circuits in dunnarts are topographically organized according to cell body position. (A to C) *In vivo* injections of retrograde tracers (cholera toxin B, CTB) into the postero-medial cortex of dunnarts, left panels, and insets of the contralateral claustrum on right panels at defined Bregma coordinates (in mm, bottom left). (A) Superposition of the experiments in A to C, indicating the approximate position of topographically segregated cell bodies in the contralateral claustrum (right panel). Ins, insular cortex; rf, rhinal fissure; WM, white matter. Scale bars: 250 μ m.

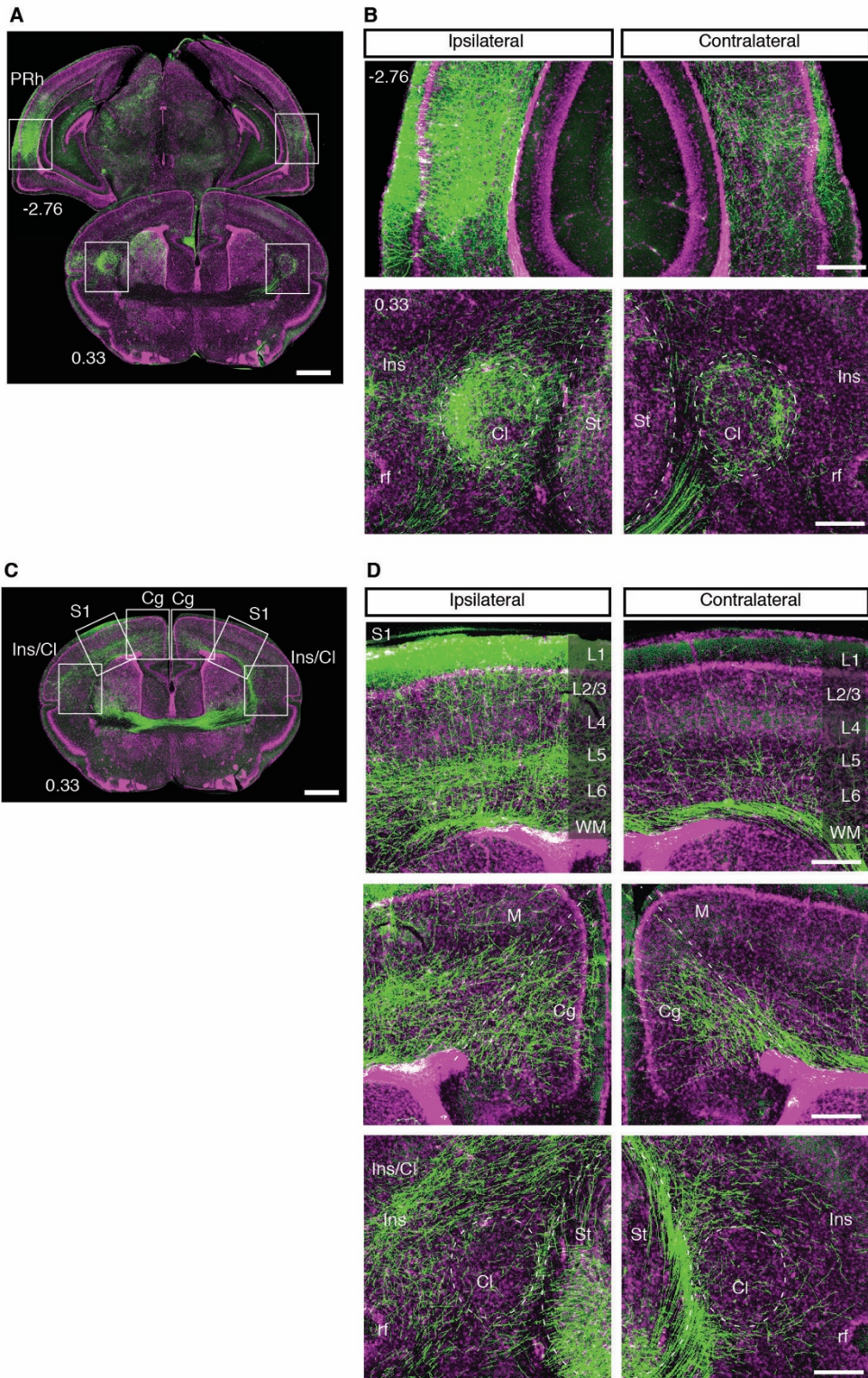


Fig. S9. Mirror ipsilateral and contralateral projections in dunnarts reveal hyperconnected hubs in medial and lateral regions of the cortex. (*A*) In-pouch electroporated neurons in the perirhinal cortex (PRh, Bregma -2.76 mm) result in contralateral projections to the homotopic region (*B*, top panels), as well as heterotopic ipsi- and contralateral projections to the claustrum (Cl, Bregma 0.33 mm; *B*, bottom panels). (*C*) Electroporation in the primary somatosensory cortex (S1, Bregma 0.33 mm) labels axonal terminals in the contralateral homotopic S1 (*D*, top panels), as well as bilateral projections to the cingulate cortices (Cg, *D*, middle panels) and insular (Ins) region, while avoiding the claustrum in both hemispheres (*D*, bottom panels). rf, rhinal fissure; St, striatum. Scale bars: 1 mm in *A*, and *C*; 250 μ m in *B* and *D*.

Areas	Individual experiments (animal id-dye)																
	393-DI	613-C5	486-C5	610-C5	534-C5	467-DD	476-DD	534-C6	610-C6	403-DI	415-DI	465-DI	451-DI	579-C6	580-C6	486-C6	613-C6
aPir	51	4	18	26	371	13	11	6	0	1	6	10	10	61	2	166	0
pPir	0	4	0	9	50	0	24	12	0	12	7	11	17	9	27	75	0
Orbl	98	55	69	92	216	54	23	13	11	0	25	0	0	82	333	88	7
Orbv	20	176	244	44	220	13	28	0	1	0	1	0	0	34	119	53	0
Orbm	8	356	120	45	211	8	9	0	0	0	5	0	0	5	3	288	0
Fr	149	280	260	343	341	88	9	7	32	0	11	0	0	76	173	17	4
aCg	2	246	35	95	755	175	129	75	61	156	49	15	16	186	96	32	2
aM	19	717	546	296	748	214	107	28	48	15	3	0	0	93	91	74	0
cM	0	4	0	65	411	175	87	248	300	22	50	12	24	215	116	2	0
aS1	7	14	21	406	1438	115	167	145	107	47	10	5	17	130	72	10	1
cS1	3	2	0	272	245	96	268	580	359	131	65	4	28	171	128	3	2
aS2	2	2	0	34	20	30	82	9	14	244	176	82	109	19	60	1	12
aIns	6	46	43	113	457	76	230	36	5	98	32	11	30	38	52	27	0
aCl	6	94	28	16	43	44	17	5	22	8	7	7	9	90	121	40	5
pCl	0	5	3	13	5	6	6	5	13	8	72	12	4	187	185	141	10
aEnd	7	2	28	2	59	12	15	1	5	1	1	3	10	19	4	10	1
pEnd	0	3	0	1	0	2	5	0	0	2	13	3	2	0	0	3	0
pCg	10	424	83	159	444	48	15	107	130	43	37	32	22	459	350	61	1
RSP/Sub	0	107	0	6	6	8	3	2	1	4	0	3	6	76	118	187	269
pM	1	0	25	69	299	15	3	149	122	8	17	20	7	325	205	19	0
pS1	11	5	0	147	118	30	24	229	257	29	162	53	74	617	699	199	25
pS2	0	3	0	44	33	9	4	7	41	39	237	198	67	15	162	224	18
pIns	4	6	1	51	218	74	122	45	31	708	235	197	65	21	80	138	15
A1/Tea	0	3	0	0	7	5	0	4	1	0	0	0	0	4	353	148	58
PRh/Ect	0	1	0	0	24	0	7	4	7	2	0	0	3	26	78	4	0
V2/Ent	0	12	0	0	1	0	0	0	1	0	0	0	0	0	119	57	403
V1	0	0	0	0	2	5	0	0	0	0	0	0	0	0	285	40	422

Injection site coverage per area:




	< 20%
	20-50%
	> 50%

Table S1. Contralateral circuit mapping in dunnarts demonstrate homotopic and

heterotopic circuits. Total count of retrogradely labeled neurons per experiment

(columns) and brain areas (rows). Site and extent of contralateral injections are shown in

green per experiment (animal number and dye used; *i.e.*, DI/DD, DiI/DiD; C5/C6, CTB

555/CTB 647). Horizontal bars (magenta) show the relative proportion of commissural

neuron count per experiment. A1/TeA, auditory cortex/ temporal association area; aCg,

anterior cingulate cortex; aCl, anterior claustrum; aEnd, anterior endopiriform nucleus;

aIns, anterior insular cortex; aM, anterior motor cortex; aPir, anterior piriform cortex;

aS1, anterior primary somatosensory cortex; aS2, anterior secondary somatosensory

cortex; cM, central motor cortex; cS1, central primary somatosensory cortex; Ent,

entorhinal cortex; Fr, frontal cortex; Orbl, lateral orbital cortex; Orbm, medial orbital

cortex; Orbv, ventral orbital cortex; pCg, posterior cingulate cortex; pCl, posterior claustrum; pEnd, posterior endopiriform nucleus; pIns, posterior insular cortex; pM, posterior motor cortex; pPir, posterior piriform cortex; PRh/Ect, perirhinal/ectorhinal area; pS1, posterior primary somatosensory cortex; pS2, posterior secondary somatosensory cortex; RSP, retrosplenial complex; Sub, subiculum; V1, primary visual cortex; V2L, secondary visual cortex lateral; V2M, secondary visual cortex medial.

Captions for Supplementary Movies

Movie S1. Segregation of homotopic domains along the anterior commissure in dunnarts. Three-dimensional animation of tractography using inclusion regions of interest (ROIs) between the anterior commissure (cyan ball) and seven small ROIs placed in different cortical areas, as indicated in Fig. 2A.

Movie S2. Topography of homotopic fibers along the platypus anterior commissure. Movement of a small region of interest (ROI; yellow sphere) within the mid-sagittal anterior commissure along the antero-posterior, dorso-ventral and oblique antero-posterior/dorso-ventral axes, as detailed in Fig. S3, results in topographic homotopic bilateral tracts (red). Coronal, horizontal and sagittal planes are shown intersecting at corresponding points of ROI movement.

Movie S3. Segregation of homotopic fibers in the anterior commissure of platypus. Three-dimensional animation of a platypus brain tractography after parcellating the mid-sagittal anterior commissure at equivalent regions to those described in Fig. 3C. Homotopic contralateral fibers include the olfactory/piriform (red), rostral cortical (orange), bulk neocortical (yellow) and entorhinal cortex (green) domains.

References

1. Suárez R, *et al.* (2017) Development of body, head and brain features in the Australian fat-tailed dunnart (*Sminthopsis crassicaudata*; Marsupialia: Dasyuridae); A postnatal model of forebrain formation. *PLoS One* 12(9):e0184450.
2. Paolino A, Fenlon LR, Kozulin P, Richards LJ, & Suárez R (2018) Multiple events of gene manipulation via in pouch electroporation in a marsupial model of mammalian forebrain development. *Journal of Neuroscience Methods* 293:45-52.
3. Ashwell KWS, McAllan BM, & Mai JK (2010) Atlas of the brain of the stripe-faced dunnart (*Sminthopsis macroura*). *The Neurobiology of Marsupials*, ed Ashwell KWS (Cambridge University Press, New York), p 241.